ACS APPLIED MATERIALS & INTERFACES

Letter

www.acsami.org

Mesoporous CoO Nanocubes @ Continuous 3D Porous Carbon Skeleton of Rose-Based Electrode for High-Performance Supercapacitor

Danni Lan,[†] Yangyang Chen,[†] Pan Chen,[†] Xuanying Chen,[†] Xu Wu,[†] Xuli Pu,[‡] Yan Zeng,[†] and Zhihong Zhu*,[†]

[†]Institute of Nano-Science and Nano-Technology, College of Physical Science and Technology, Central China Normal University, Wuhan 430079, P. R. China

[‡]Xiamen Entry-Exit Inspection and Quarantine Bureau of the People's Republic of China, Xiamen 36102, P. R. China

Supporting Information

ABSTRACT: Supercapacitors have attracted lots of attentions for energy storage because of their outstanding electrochemical properties, and various kinds of carbon materials have been used to improve the performance. In this work, we innovatively elevate a natural rose-based continuous 3D porous carbon skeleton. The as-prepared carbon skeleton is graphited to some extent and possesses hierarchical interconnected 3D porous structures, providing a high electrical conductive and electrolyte easy-infiltrated substrate for the fabrication of ideal monolithic composite electrodes. Then, we utilized it as scaffold to prepare mesoporous CoO nanocubes @ continuous 3D porous carbon skeleton of rose composite-based electrode for supercapacitor via hydrothermal approach. The obtained material exhibits a noticeable pseudocapacitive performance with a brilliant capacitance of 1672 F/g at 1 A/g and as high as 521 F/g at 40 A/g. It also should be noted that ~82% of the capacitance was maintained after 3000 cycles at 5 A/g, and only 40% capacitance loss after 1500 cycles at a relatively high current density of 10 A/g.

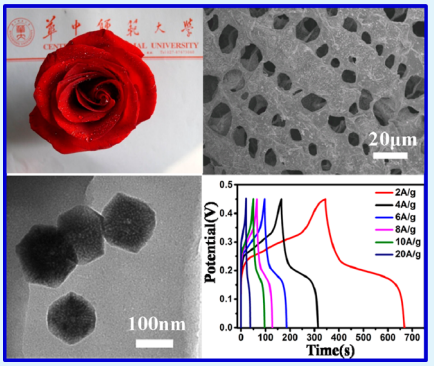

KEYWORDS: *carbon skeleton of rose, mesoporous CoO nanocubes, hydrothermal reaction, supercapacitor, electrochemical performance*

INTRODUCTION

The increasing energy demand and environmental pollution call for not only urgent development of clean energies and effective control of the pollutant emissions but also more efficient energy storage devices.[1,2] Great efforts have been made on it;[3−7] until now, electrochemical supercapacitors (electric double layer capacitors (EDLCs) and pseudocapacitiors) have gradually moved onto the stage of business, and showed an immense potential.[8−13] Because of the ion adsorption mechanism, the specific capacitances of EDLCs are limited (lower than 300 F/g for carbon-based EDLCs).[14−16] On the other hand, pseudocapacitors based on the storage mechanism of redox reactions always have a preponderant energy density. If their power density and cycling stability can be improved to a high level, it will definitely show great superiority for energy storage than EDLCs.[17,18] Many transition metal oxides or hydroxides and conducting polymers have been chosen as electrode materials to increase the storage performance of pseudocapacitors, such as RuO_2,[19] $Ni(OH)_2$,[20] MnO_2,[21] PEDOT,[22] PANI,[23] etc. However, they're still defective for the relatively low rate performance and stability. As for costs, some of them are restricted only to few applications.[24] Among these materials, cobalt oxides are relatively cheap pseudocapacitor materials with high theoretical capacitance, and have attracted many attentions.[25−27] A lot of research has been reported on Co_3O_4, but less has been reported about CoO. According to the theoretical capacitances, the theoretical capacitance of pure CoO and Co_3O_4 are 4292[28] and 3560[29] F/g, respectively, which indicates CoO can be a better candidate for pseudocapacitor electrode material than Co_3O_4. For transition metal oxide electrode materials, they always suffer from poor electrical/ionic conductivity, so the most important issue in designing these electrode materials is to provide high ways for electron delivery and ion diffusion. One of the effective ways to solve this problem is incorporation of nanosized metal oxides with a carbon-based material, using the unique nanostructure to enhance the ion diffusion and utilizing electrically conductive carbon framework to accelerate the electron transfer. For instance, CoO nanoflowers woven by CNT network,[30] 3D graphene,supported cobalt oxide,[31] or Co_3O_4 nanowires grown on carbon fiber paper,[32] etc. have been successfully applied on pseudocapacitor and have shown excellent electrochemical performances.

In this work, we originally synthesized mesoporous CoO nanocubes @ continuous 3D porous carbon skeleton of rose composite. In particular, we creatively obtained the continuous

Received: May 29, 2014
Accepted: July 28, 2014
Published: July 28, 2014

   dx.doi.org/10.1021/am503378n | ACS Appl. Mater. Interfaces 2014, 6, 11839−11845

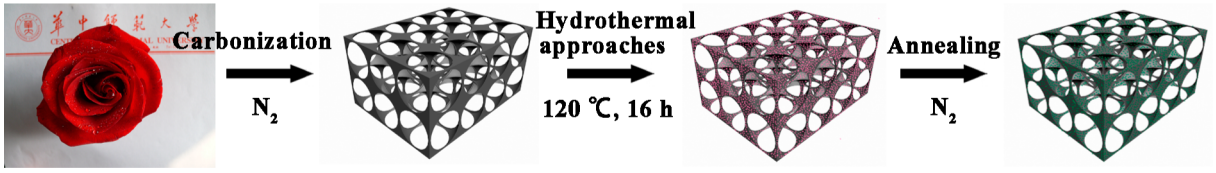

Figure 1. Illustration of the synthesis path of mesoporous CoO nanocubes @ continuous 3D porous carbon skeleton of rose.

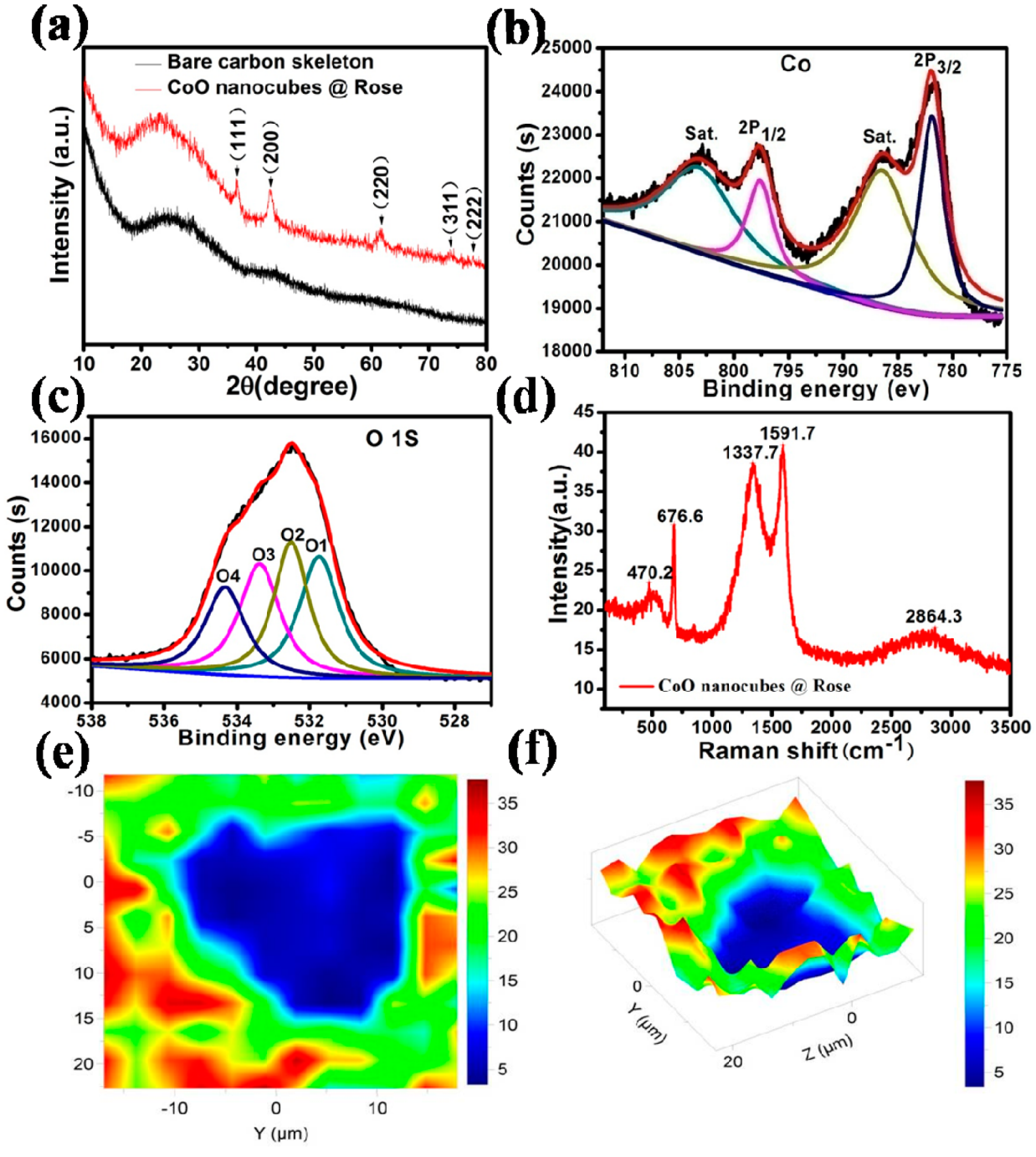

Figure 2. (a) XRD patterns, (b, c) XPS spectra, (d) Raman spectrum, and (e, f) 2D and 3D Raman mapping images (the blue shows pores, the green represents the G band of graphite, and the red indicates Co−O band) of the mesoporous CoO nanocubes @ continuous 3D porous carbon skeleton of rose.

3D network structured carbon skeleton from the abundant flower of rose just through a simple nitrogen atmosphere protected carbonization process without any other reagents for assistance for the first time. The cost is small and the concept is quite eco-friendly. The as-prepared carbon skeleton is graphited and possesses hierarchical interconnected 3D porous structures.

dx.doi.org/10.1021/am503378n | ACS Appl. Mater. Interfaces 2014, 6, 11839−11845

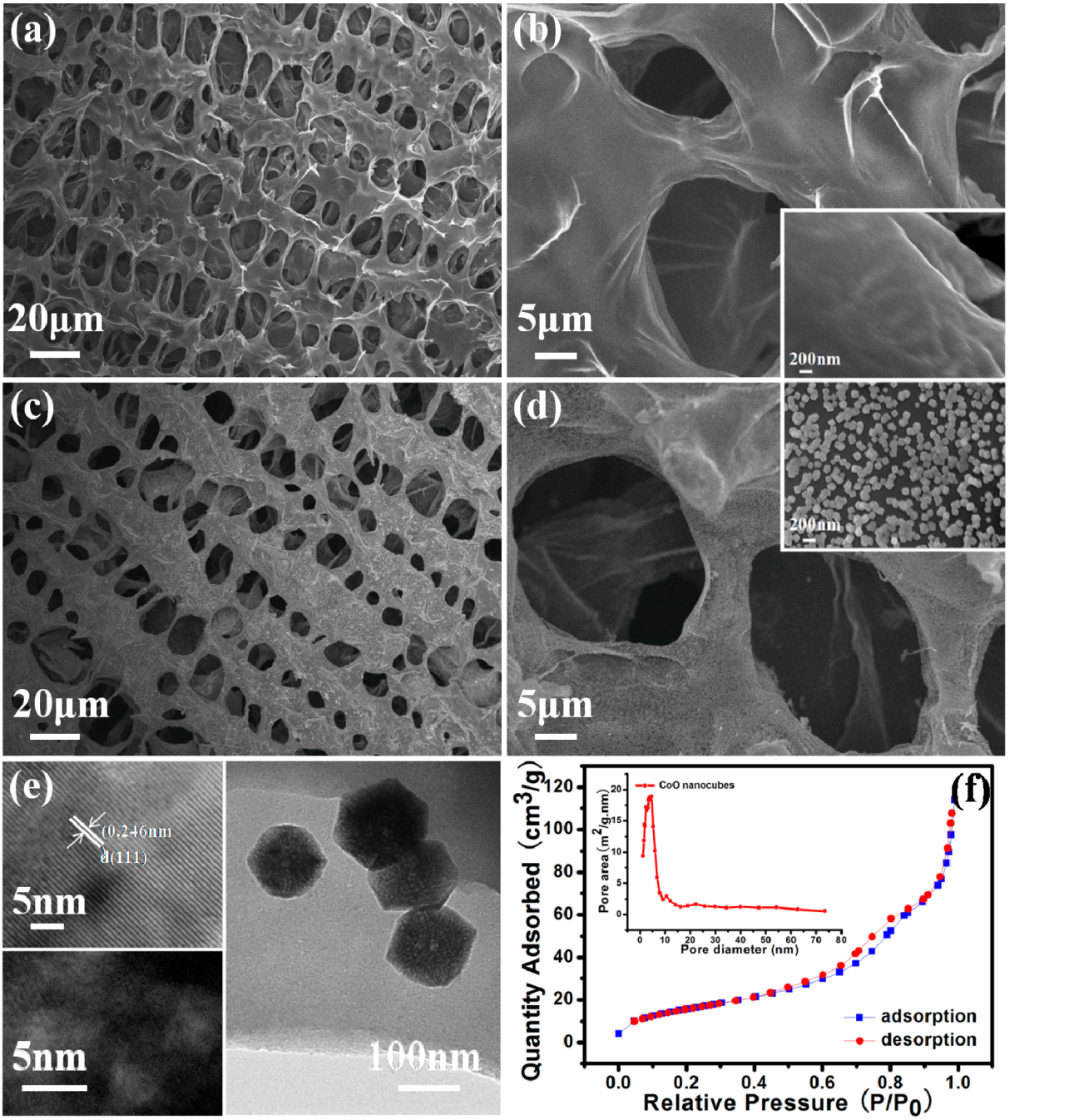

Figure 3. SEM images of (a, b) bare carbon skeleton of rose and (c, d) composite of mesoporous CoO nanocubes @ continuous 3D porous carbon skeleton of rose at different magnification. (e) HRTEM image of the composite, where the insets are HRTEM images of a single CoO nanocube. (f) N_2 adsorption−desorption isotherm and (inset in f) PSD of the mesoporous CoO nanocubes.

When used on pseudocapacitior electrode material, it can provide a high electrical conductive and electrolyte easily infiltrated substrate for the mesoporous CoO nanocubes, eventually leading to the effective acceleration of electron transfer and shortening of ion diffusion path. Besides, the unique mesoporous structure of CoO nanocubes not only favors the electrolytes diffusion that can accelerate the facility of ion transportation but also ensures the high utilization of electrode material. At last, the composite exhibits an excellent electrochemical property with a brilliant capacitance of 1672 F/g at 1 A/g and as high as 521 F/g at 40 A/g, about 82% of the capacitance was maintained after 3000 cycles at 5 A/g and only 40% capacitance loss after 1500 cycles at a relatively high current density of 10 A/g. We demonstrate that the unique structure of the porous carbon-based nanocomposite can accommodate the electroactive species accessible to fast faradaic reactions in bulk electrode materials, which shows better rate capability and great potential as electrode materials for supercapacitors.

RESULTS AND DISCUSSION

Schematic illustration of the synthesis process is shown in Figure 1. First, the graphitized 3D porous carbon substrate can be obtained by the pretreated and the following nitrogen protected carbonization of fresh rose. Then, via a hydrothermal

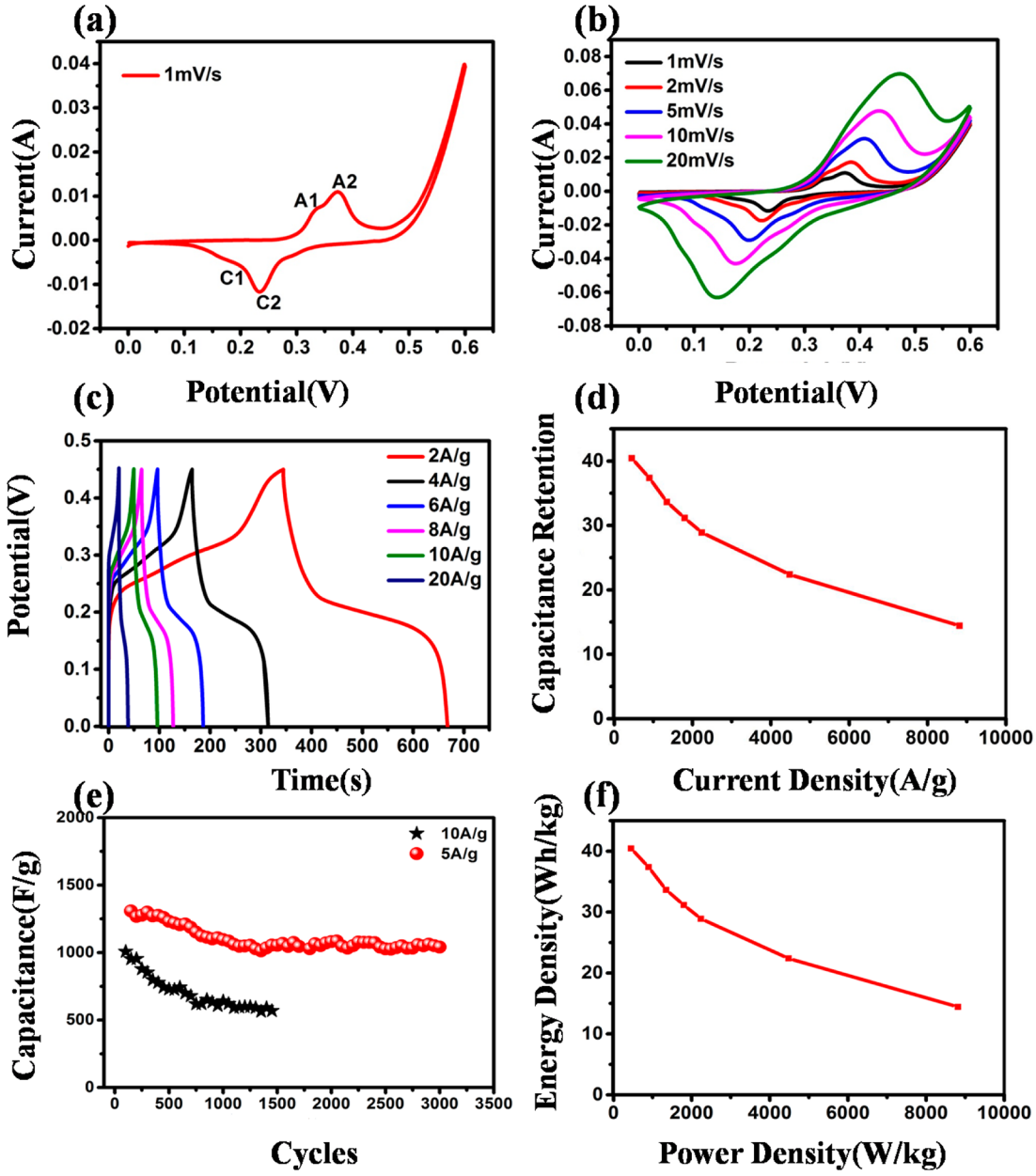

Figure 4. (a) CV curves of the mesoporous CoO nanocubes @ continuous 3D porous carbon skeleton of rose at a scan rate of 1 mV/s; (b) CV curves at different scan rates; (c) galvanostatic charge−discharge curves of the mesoporous CoO nanocubes @ continuous 3D porous carbon skeleton of rose based electrode at different current densities; (d) corresponding specific capacitances at different discharging current densities; (e) cycling performance of the mesoporous CoO nanocubes @ continuous 3D porous carbon skeleton of rose at 10 A/g and 5 A/g; (f) Ragone plot of the prepared mesoporous CoO nanocubes @ continuous 3D porous carbon skeleton of rose.

method, the pink colored cobalt carbonate hydroxides were attached onto the carbon scaffold. After an annealing process, we finally synthesized the mesoporous CoO nanocubes @ continuous 3D porous carbon skeleton of rose composite with a dark green look.

A feasible growth mechanism of the cubic CoO can be given as follow:[33]

$$Co^{2+} + xF^- \rightarrow [CoFx]^{(x-2)^-} \quad (4)$$

$$H_2NCONH_2 + H_2O \rightarrow 2NH_3 + CO_2 \quad (5)$$

$$CO_2 + H_2O \rightarrow CO_3^{2-} + 2H^+ \quad (6)$$

$$NH_3{\cdot}H_2O \rightarrow NH_4^+ + OH^- \quad (7)$$

$$[CoF_x]^{(x-2)-} + 0.5(2-y)CO_3^{2-} + yOH^- + nH_2O \rightarrow Co(OH)_y(CO_3)_{0.5(2-y)}{\cdot}nH_2O + xF^- \quad (8)$$

$$Co(OH)_y(CO_3)_{0.5(2-y)}{\cdot}nH_2O \rightarrow CoO + (3n + 1.5y)H_2O + 1.5(2-y)CO_2 \quad (9)$$

The X-ray diffraction (XRD) pattern of the composite of mesoporous CoO nanocubes @ continuous 3D porous carbon skeleton of rose is shown in Figure 2a, where five obvious diffraction peaks coincide with the (111), (200), (220), (311) and (222) planes of standard spectrum of cubic CoO (JCPDS42−1467).[34] Compared with the black XRD curve of bare carbon skeleton, it can be confirmed that the mesoporous

CoO nanocubes were successfully compounded with continuous 3D porous carbon skeleton of rose without any other impurity. The more detailed elemental composition and valence state of CoO nanocubes are further characterized by XPS measurements and the results are presented in Figure 2b, c. In the Co 2P region (Figure 2b), two main peaks with obvious satellite peaks (satellites: 785.9 and 802.9 eV) corresponding to the Co $2P_{3/2}$ (781.4 eV) and Co $2P_{1/2}$ (797.9 eV) levels are observed, and from Figure 2c we can see the O 1S region contains a O4 peak at the higher value of 531.7 eV, which particularly verifies the existence of CoO.[34−36] Furthermore, the as-synthesized sample was examined by Raman spectra, shown in Figure 2d. It exhibits five obvious peaks that correspond to Raman active vibrational modes of Co−O and graphite. In detail, peaks at 468.3 and 674.7 cm^{-1} are classical vibration modes of Co−O,[37−39] which agree with the XPS analysis, whereas the other three peaks at 1337.7, 1591.7, and 2864.3 cm^{-1} refer to the D, G, and 2D peaks, further confirming that the carbon skeletons we prepared are graphitized to some extent and have strong electrical conductivity. Panels e and f in Figure 2 illustrate the 2D and 3D visual Raman mappings of the obtained composite, where the blue shows pores, the green represents the typical Raman peaks of G band for graphite and the red indicates classical vibration modes of Co−O, which can be clearly seen that the CoO was grown on the carbon material directly.[40]

Images a and b in Figure 3 shows SEM images of the as-prepared carbon scaffold under different magnifications. It can be observed that the carbon scaffold has a continuous 3D porous structure. All the pores in the carbon scaffold, whether on surface or in the inner space, are connected with each other and reached out in all directions to form the ordered 3D porous network, resulting in enough channels for electrolyte going through. At the same time, the surfaces of the skeleton are wavy and crinkly, which can effectively increases the surface area of the carbon scaffold. SEMs of the product after hydrothermal reaction can be seen from Figure 3c, d. It can be found that the continuous 3D porous structure of the carbon scaffold of rose kept well, which means the porous structure of our carbon substrate is very stable. Meanwhile, regular cubic CoO is shown directly grown on the whole surface of the substrate densely and evenly with the dimension of ∼100 nm. In fact, the size of the cubic CoO can be easily controlled in our experiments by changing the reaction concentrations of the precursor of $Co(NO_3)_2{\cdot}6H_2O$, with the concentration of no more than 10 mM, the higher concentration will give a larger size. It can also be acknowledged that almost every nanocube distributes independently, which can be attributed to the stereochemical effect of CTAB,[41] without which the nanocubes will connected together with each other (see Figure S1 in the Supporting Information). TEM is further used to characterize the products. Wrinkled surfaces of the rose carbon skeleton as well as the homogeneous nanocubic structure can be clearly seen from Figure S2 in the Supporting Information, whereas the selected area electron diffraction (SAED) patterns in inset give the polycrystalline nature of the cubic CoO. Insets of Figure 3e clearly exhibited the mesoporous structure of the CoO nanocube with the mesopores size of about 5 nm and the lattice space of 0.246 nm referring to the (111) interplanar distance of CoO. To investigate the mesoporosity of CoO, we show the N_2 adsorption−desorption isotherm and pore size distributions (PSD) in Figure 3f, where the hysteresis loop in CoO nanocubes reveals a narrow distribution of pore size.[42] The average pore size is about 5 nm as demonstrated in the inset in Figure 3f, corresponding to the TEM image in Figure 3e. Moreover, mesoporous CoO nanocubes possess a BET surface area of 59 m^2/g, which is higher than reported before.[43] As a consequence, it is quite reasonable to expect that our as-prepared mesoporous CoO nanocubes have an excellent electrochemical performance benefiting from the sufficient redox reaction with electrolyte.

Then we employed cyclic voltammetry (CV) measurement in 2 M KOH with a three-electrode system to study the electrochemical property of the obtained composite of mesoporous CoO nanocubes @ continuous 3D porous carbon skeleton of rose. CV curve at scan rate of 1 mVs^{-1} in Figure 4a obviously shows two redox peak pairs. The redox couple of A1, C1 is due to the conversion between Co^{2+}/Co^{3+}, while the couple of A2, C2 is corresponding to the Co^{3+}/Co^{4+} reaction.[28] The CV shapes change little as the scan rates increase (Figure 4b), implying the good rate performance of the electrode,[34] which would be due to the 3D porous carbon scaffold as well as the mesoporous structure of CoO nanocubes that give the composite an excellent electron conductivity and provides high ways for ion diffusion. The galvanostatic charge−discharge (CD) curves at different current densities are given in Figure 4c, capacitances of 1438, 1328, 1195, 1108, 1025, and 788 F/g are obtained at current densities of 2, 4, 6, 8, 10, 20 A/g, respectively. With the increase of current densities from 2 to 10 A/g (Figure 4d), the specific capacitance maintains 71% of the initial value; even further enhancing the current density to 40 A/g, a specific capacitance of 521 F/g can still be obtained (see Figure S3 in the Supporting Information). To highlight the advantage of direct growth of our as-prepared mesoporous CoO nanocubes @ continuous 3D porous carbon skeleton of rose, we also performed an electrochemical test with the physical mixture of presynthesized CoO and carbon scaffold-based electrode for comparison (see Figure S4 in the Supporting Information), which confirms the high performance of our as-synthesized materials. Moreover, to estimate the capacity contribution of the current collector of nickel foam, we respectively carried out CV and galvanostatic charge−discharge measurements under the same circumstances on bare nickel foam and the obtained composite. The results shown in Figure S4 in the Supporting Information reveal that almost no capacitance contribution of nickel foam to the as-prepared product based electrode. The good cycle stability of the prepared mesoporous CoO nanocubes @ continuous 3D porous carbon skeleton of rose is further confirmed by the long-term cycling test (Figure 4e). At a high current density of 5 A/g, about 82% of the initial capacitance was retained after 3000 cycles; even at a wild higher density of 10 A/g, capacitance retention of about 60% can still be achieved after 1500 cycles. Moreover, the SEM image (see Figure S5 in the Supporting Information) of our materials after 3000 cycles demonstrates that the morphology and structure of CoO nanocubes can be largely retained with only slight aggregation after the long time process of charging/discharging, which contributes to the 82% capacitance retention.[44] Of course, it can be seen that the structure of CoO nanocubes collapsed to some degree, which would affect its redox reaction efficiency, leading to the capacitance loss finally. Figure 4f gives the Ragone plot of the supercapacitor based on the obtained product, an energy density can reaches as high as 15 Wh/kg at a high power density of 9 kW/kg. These high capacitances and such excellent high-rate and cycling performance are much

better than previously reported values,[45] even the other cobalt oxides, such as mesoporous Co_3O_4 composites.[46]

This enhanced capacitative performance of the obtained product is ascribed to the following benefits: On one hand, the open geometry of the continuous 3D porous carbon scaffold of rose and the mesopores existing in the nanocubes allow easier electrolyte penetration into the inner region of the electrode and the CoO nanocubes, and CoO can be highly exposed to and accessible by electrolyte, resulting in the low internal resistance and faster kinetics of the ion diffusion; On the other hand, the CoO nanocubes are directly grown on the continuous porous carbon scaffold of rose, leading to a splendid electrical conductivity between the CoO nanocubes and the substrate, which together with the monolithic and highly graphited carbon scaffold substrate can provide a superfast route for the electron transfer. All in all, it is the perfect combination of the mesoporous CoO and continuous 3D porous carbon scaffold of rose that lead to a very fast ion diffusion and electron transfer kinetics of the whole electrode and result in such high performances.

CONCLUSION

In summary, we successfully demonstrated mesoporous CoO nanocubes @ continuous 3D porous carbon skeleton of rose based electrode through a facile and green approach for pseudocapacitor with high capacitance and good rate capability as well as the cyclic stability. Besides the mesoporous structure of CoO nanocubes, the carbon scaffold also has an important contribution to the high performance because of its continuous 3D porous structure and good conductivity. It is novel and environmentally friendly for us to use this natural floristic carbon skeleton of rose. As proven by the highly synergistic effect above, this carbon material may take the place of the artificial synthesized complex. With further research, the other application potentials of this carbon material will emerge. Our work actually provides a method to the applications of natural floristic carbon skeleton as a substrate for constructing high-performance supercapacitors.

ASSOCIATED CONTENT

Supporting Information

Experimental details and additional supporting data such as the morphology of CoO nanocubes without CTAB, TEM image of composite, CV and CD curves at the current density of 40 A/g, electrochemical investigation of bare nickel foam as well as physical mixture of presynthesized CoO and carbon scaffold, SEM image of samples after 3000 cycles. This material is available free of charge via the Internet at http://pubs.acs.org.

AUTHOR INFORMATION

Corresponding Author

*E-mail: zhzhu@phy.ccnu.edu.cn.

Author Contributions

D.L. and Y.C. contributed equally to this work.

Notes

The authors declare no competing financial interest.

ACKNOWLEDGMENTS

This work was financially supported by self-determined research funds of CCNU from the colleges' basic research and operation of MOE (CCNU13A05007), the Key Scientific Project of Wuhan City (2013011801010598), the Scientific Project of AQSIQ (2013IK093), Foundation of National Science Talent Training Base in Physics (J1210068), and the National Natural Science Foundation of China (50802032).

REFERENCES

(1) Aricò, A. S.; Bruce, P.; Scrosati, B.; Tarascon, J.-M.; Van Schalkwijk, W. Nanostructured Materials for Advanced Energy Conversion and Storage Devices. *Nat. Mater.* **2005**, *4* (5), 366−377.

(2) Xia, X.; Chao, D.; Fan, Z.; Guan, C.; Cao, X.; Zhang, H.; Fan, H. J. A New Type of Porous Graphite Foams and Their Integrated Composites with Oxide/Polymer Core/Shell Nanowires for Supercapacitors: Structural Design, Fabrication, and Full Supercapacitor Demonstrations. *Nano Lett.* **2014**, *14* (3), 1651−1658.

(3) Chmiola, J.; Largeot, C.; Taberna, P.-L.; Simon, P.; Gogotsi, Y. Monolithic Carbide-Derived Carbon Films for Micro-Supercapacitors. *Science* **2010**, *328* (5977), 480−483.

(4) Sun, W.; Chen, X. Fabrication and Tests of a Novel Three Dimensional Micro Supercapacitor. *Microelectron. Eng.* **2009**, *86* (4), 1307−1310.

(5) Liu, C.; Li, F.; Ma, L. P.; Cheng, H. M. Advanced Materials for Energy Storage. *Adv. Mater.* **2010**, *22* (8), E28−E62.

(6) Poizot, P.; Laruelle, S.; Grugeon, S.; Dupont, L.; Tarascon, J. Nano-sized Transition-Metal Oxides as Negative-Electrode Materials for Lithium-ion Batteries. *Nature* **2000**, *407* (6803), 496−499.

(7) Lee, S. W.; Gallant, B. M.; Byon, H. R.; Hammond, P. T.; Shao-Horn, Y. Nanostructured Carbon-Based Electrodes: Bridging the Gap Between Thin-film Lithium-ion Batteries and Electrochemical Capacitors. *Energy Environ. Sci.* **2011**, *4* (6), 1972−1985.

(8) Zhang, J.; Zhao, X. On the Configuration of Supercapacitors for Maximizing Electrochemical Performance. *ChemSusChem* **2012**, *5* (5), 818−841.

(9) Miller, J. R.; Simon, P. Electrochemical Capacitors for Energy Management. *Sci. Mag.* **2008**, *321* (5889), 651−652.

(10) Stoller, M. D.; Ruoff, R. S. Best Practice Methods for Determining an Electrode Material's Performance for Ultracapacitors. *Energy Environ. Sci.* **2010**, *3* (9), 1294−1301.

(11) Wei, T. Y.; Chen, C. H.; Chien, H. C.; Lu, S. Y.; Hu, C. C. A Cost−Effective Supercapacitor Material of Ultrahigh Specific Capacitances: Spinel Nickel Cobaltite Aerogels from an Epoxide−Driven Sol−Gel Process. *Adv. Mater.* **2010**, *22* (3), 347−351.

(12) Lota, G.; Fic, K.; Frackowiak, E. Carbon Nanotubes and Their Composites in Electrochemical Applications. *Energy Environ. Sci.* **2011**, *4* (5), 1592−1605.

(13) Jayalakshmi, M.; Balasubramanian, K. Simple Capacitors to Supercapacitors-An Overview. *Int. J. Electrochem. Sci.* **2008**, *3* (11), 1196−1217.

(14) Cao, X.; Shi, Y.; Shi, W.; Lu, G.; Huang, X.; Yan, Q.; Zhang, Q.; Zhang, H. Preparation of Novel 3D Graphene Networks for Supercapacitor Applications. *Small* **2011**, *7* (22), 3163−3168.

(15) Simon, P.; Gogotsi, Y. Materials for Electrochemical Capacitors. *Nat. Mater.* **2008**, *7* (11), 845−854.

(16) Li, H.; Yu, M.; Lu, X.; Liu, P.; Liang, Y.; Xiao, J.; Tong, Y.; Yang, G. Amorphous Cobalt Hydroxide with Superior Pseudocapacitive Performance. *ACS Appl. Mater. Interfaces* **2014**, *6* (2), 745−749.

(17) Lang, X.; Hirata, A.; Fujita, T.; Chen, M. Nanoporous Metal/Oxide Hybrid Electrodes for Electrochemical Supercapacitors. *Nat. Nanotechnol.* **2011**, *6* (4), 232−236.

(18) Yang, L.; Cheng, S.; Ding, Y.; Zhu, X.; Wang, Z. L.; Liu, M. Hierarchical Network Architectures of Carbon Fiber Paper Supported Cobalt Oxide Nanonet for High-Capacity Pseudocapacitors. *Nano Lett.* **2011**, *12* (1), 321−325.

(19) Wu, X.; Zeng, Y.; Gao, H.; Su, J.; Liu, J.; Zhu, Z. Template Synthesis of Hollow Fusiform $RuO_2 \cdot xH_2O$ Nanostructure and Its Supercapacitor Performance. *J. Mater. Chem. A* **2013**, *1* (3), 469−472.

(20) Wang, H.; Casalongue, H. S.; Liang, Y.; Dai, H. $Ni(OH)_2$ Nanoplates Grown on Graphene as Advanced Electrochemical Pseudocapacitor Materials. *J. Am. Chem. Soc.* **2010**, *132* (21), 7472−7477.

(21) Park, S.; Nam, I.; Kim, G.-P.; Han, J. W.; Yi, J. Hybrid MnO_2 Film with Agarose Gel for Enhancing the Structural Integrity of Thin Film Supercapacitor Electrodes. *ACS Appl. Mater. Interfaces* **2013**, *5* (20), 9908−9912.
(22) Carlberg, J.; Inganäs, O. Poly (3, 4−ethylenedioxythiophene) as Electrode Material in Electrochemical Capacitors. *J. Electrochem. Soc.* **1997**, *144* (4), L61−L64.
(23) Fusalba, F.; Gouérec, P.; Villers, D.; Bélanger, D. Electrochemical Characterization of Polyaniline in Nonaqueous Electrolyte and Its Evaluation as Electrode Material for Electrochemical Supercapacitors. *J. Electrochem. Soc.* **2001**, *148* (1), A1−A6.
(24) Lou, X. W. D. Growth of Ultrathin Mesoporous Co_3O_4 Nanosheet Arrays On Ni Foam for High-Performance Electrochemical Capacitors. *Energy Environ. Sci.* **2012**, *5* (7), 7883−7887.
(25) Meher, S. K.; Rao, G. R. Ultralayered Co_3O_4 for High-Performance Supercapacitor Applications. *J. Phys. Chem. C* **2011**, *115* (31), 15646−15654.
(26) Chen, J. S.; Zhu, T.; Hu, Q. H.; Gao, J.; Su, F.; Qiao, S. Z.; Lou, X. W. Shape-Controlled Synthesis of Cobalt-Based Nanocubes, Nanodiscs, and Nanoflowers and Their Comparative Lithium-Storage Properties. *ACS Appl. Mater. Interfaces* **2010**, *2* (12), 3628−3635.
(27) Xia, X.-H.; Tu, J.-P.; Wang, X.-L.; Gu, C.-D.; Zhao, X.-B. Mesoporous Co_3O_4 Monolayer Hollow-Sphere Array as Electrochemical Pseudocapacitor Material. *Chem. Commun.* **2011**, *47* (20), 5786−5788.
(28) Zhou, C.; Zhang, Y.; Li, Y.; Liu, J. Construction of High-Capacitance 3D CoO @ Polypyrrole Nanowire Array Electrode for Aqueous Asymmetric Supercapacitor. *Nano Lett.* **2013**, *13* (5), 2078−2085.
(29) Xiao, Y.; Liu, S.; Li, F.; Zhang, A.; Zhao, J.; Fang, S.; Jia, D. 3D Hierarchical Co_3O_4 Twin−Spheres with an Urchin−Like Structure: Large−Scale Synthesis, Multistep−Splitting Growth, and Electrochemical Pseudocapacitors. *Adv. Funct. Mater.* **2012**, *22* (19), 4052−4059.
(30) Zhu, Y. G.; Wang, Y.; Shi, Y.; Wong, J. I.; Yang, H. Y. CoO Nanoflowers Woven by CNT Network for High Energy Density Flexible Micro-Supercapacitor. *Nano Energy* **2014**, *3*, 46−54.
(31) Dong, X.-C.; Xu, H.; Wang, X.-W.; Huang, Y.-X.; Chan-Park, M. B.; Zhang, H.; Wang, L.-H.; Huang, W.; Chen, P. 3D Graphene−Cobalt Oxide Electrode for High-Performance Supercapacitor and Enzymeless Glucose Detection. *ACS Nano* **2012**, *6* (4), 3206−3213.
(32) Rakhi, R.; Chen, W.; Cha, D.; Alshareef, H. Substrate Dependent Self-Organization of Mesoporous Cobalt Oxide Nanowires with Remarkable Pseudocapacitance. *Nano Lett.* **2012**, *12* (5), 2559−2567.
(33) Xia, X.-h.; Tu, J.-p.; Zhang, Y.-q.; Mai, Y.-j.; Wang, X.-l.; Gu, C.-d.; Zhao, X.-b. Freestanding Co_3O_4 Nanowire Array for High Performance Supercapacitors. *Rsc Adv.* **2012**, *2* (5), 1835−1841.
(34) Jiang, L.; Zou, R.; Li, W.; Sun, J.; Hu, X.; Xue, Y.; He, G.; Hu, J. Ni $(OH)_2$/CoO/Reduced Graphene Oxide Composites with Excellent Electrochemical Properties. *J. Mater. Chem. A* **2012**, *1* (3), 478−481.
(35) Wang, H.; Qing, C.; Guo, J.; Aref, A.; Sun, D.; Wang, B.; Tang, Y. Highly Conductive Carbon-CoO Hybrid Nanostructured Arrays with Enhanced Electrochemical Performance for Asymmetric Supercapacitors. *J. Mater. Chem. A* **2014**, *2*, 11776−11783.
(36) Sexton, B.; Hughes, A.; Turney, T. An XPS and TPR Study of the Reduction of Promoted Cobalt-Kieselguhr Fischer−Tropsch Catalysts. *J. Catal.* **1986**, *97* (2), 390−406.
(37) Wang, W.; Zhang, G. Synthesis and Optical Properties of High-Purity CoO Nanowires Prepared by an Environmentally Friendly Molten Salt Route. *J. Cryst. Growth* **2009**, *311* (17), 4275−4280.
(38) Tang, C.-W.; Wang, C.-B.; Chien, S.-H. Characterization of Cobalt Oxides Studied by FT-IR, Raman, TPR and TG-MS. *Thermochim. Acta* **2008**, *473* (1), 68−73.
(39) Choi, H. C.; Jung, Y. M.; Noda, I.; Kim, S. B. A Study of the Mechanism of the Electrochemical Reaction of Lithium with CoO by Two-Dimensional Soft X-ray Absorption Spectroscopy (2D XAS), 2D Raman, and 2D Heterospectral XAS-Raman Correlation Analysis. *J. Phys. Chem. B* **2003**, *107* (24), 5806−5811.
(40) Gouadec, G.; Colomban, P. Raman Spectroscopy of Nanomaterials: How Spectra Relate to Disorder, Particle Size and Mechanical Properties. *Prog. Cryst. Growth Charact. Mater.* **2007**, *53* (1), 1−56.
(41) Guo, C.; Zhang, X.; Huo, H.; Xu, C.; Han, X. Co_3O_4 Microspheres with Free-Standing Nanofibers for High Performance Non-Enzymatic Glucose Sensor. *Analyst* **2013**, *138* (22), 6727−6731.
(42) Kim, S.-I.; Lee, J.-S.; Ahn, H.-J.; Song, H.-K.; Jang, J.-H. Facile Route to an Efficient NiO Supercapacitor with a Three-Dimensional Nanonetwork Morphology. *ACS Appl. Mater. Interfaces* **2013**, *5* (5), 1596−1603.
(43) Sun, Y.; Hu, X.; Luo, W.; Huang, Y. Self-assembled Mesoporous CoO Nanodisks as a Long-Life Anode Material for Lithium-ion Batteries. *J. Mater. Chem.* **2012**, *22* (27), 13826−13831.
(44) Zhang, G. Q.; Wu, H. B.; Hoster, H. E.; Chan-Park, M. B.; Lou, X. W. D. Single-Crystalline $NiCo_2O_4$ Nanoneedle Arrays Grown on Conductive Substrates as Binder-Free Electrodes for High-Performance Supercapacitors. *Energy Environ. Sci.* **2012**, *5* (11), 9453−9456.
(45) JináFan, H. Hybrid Structure of Cobalt Monoxide Nanowire @ Nickel Hydroxidenitrate Nanoflake Aligned on Nickel Foam for High-Rate Supercapacitor. *Energy Environ. Sci.* **2011**, *4* (11), 4496−4499.
(46) Liu, X.; Long, Q.; Jiang, C.; Zhan, B.; Li, C.; Liu, S.; Zhao, Q.; Huang, W.; Dong, X. Facile and Green Synthesis of Mesoporous Co_3O_4 Nanocubes and Their Applications for Supercapacitors. *Nanoscale* **2013**, *5* (14), 6525−6529.